



Half-plane contact problems in partial slip with varying normal and tangential loads

J.P.J. Truelove^{*}, L.E. Blades, D.A. Hills

Department of Engineering Science, University of Oxford, Parks Road, Oxford, OX1 3PJ, UK

ARTICLE INFO

Keywords:

Contact mechanics
Partial slip
Half plane

ABSTRACT

Simple methods of finding the transient and steady state stick zones for frictional contacts subject to varying normal and shear forces are discussed. Particular emphasis is given to the Hertzian contact because the algebra is very simple for this geometry, but the methods and results may be carried over to any other contact geometry that can be solved within the framework of half plane theory, including the widely-occurring flat contact with radiused edges.

1. Introduction

The study of frictional, notionally static contacts subject to varying loads is important because they provide both frictional damping which controls the amplitude of vibrations in mechanical assemblies, and provide an environment which potentially leads to the nucleation of cracks. For many years studies of these problems were confined to cases where the normal load remained constant, from the seminal paper of Cattaneo (1938) right through to 2011, when Barber et al. (2011) looked at the complicated case of a contact subject to harmonically varying normal and shear forces, of the same frequency, but with an arbitrary phase shift. It is certainly the case that this analysis is of practical value, as there are problems, such as eccentric weights on rotating shafts, which give rise to loads varying in this manner, but it is equally true that there are many problems where one external load induces changes in both normal and shear forces (which must therefore necessarily be in phase), and a second external load induces changes in the normal and shear forces, but in a different ratio. For example, in a wellhead riser clamp one external force could be the clamping force, hydraulically applied, and the other might be riser drift due to wave forces.

We have recently given attention to a number of contacts in which the contact supported a moment and normal force and the shear tractions present were excited by both a shear force and differential tension in the surfaces of the bodies (Andresen et al., 2019, 2020), in the steady state, but the formulations used avoided the need to look at the traction evolution. This is an illuminating way of looking at the problems, and is the subject of this paper. The study is restricted to uncoupled half-plane contacts, so that normal tractions induce no relative slip between surface particles, and shear tractions induce no

relative normal displacement of surface particles. Usually, the absence of coupling is achieved by requiring both bodies to be made from the same material. We restrict attention to problems where the contact is symmetric and of half width a , the normal load is P and the shear force present is Q . The load history will be displayed in $P-Q$ space and the coefficient of friction between the bodies is μ . It is tempting to infer that the lack of coupling in the solution means that the state of stress (and in particular, the traction distribution) present is independent of the loading path taken, but this is not so. It is true that the contact pressure distribution is independent of the loading trajectory, because the relative curvature of the bodies is unaffected by the shear tractions. On the other hand, if the normal load is increasing the contact patch is also gradually increasing in size, and the shearing tractions being developed will change in proportion to the change in normal load.

The starting point for these results is the observation that the Green's functions for normal and shear line forces (P, Q) on the surface of a half-plane produce the same corresponding surface displacements ($v(x), u(x)$). This result

$$\frac{v(x)}{P} = \frac{u(x)}{Q} \quad (1)$$

comes straight from Flamant's solution. It follows that, if we have similar *distributions* of direct and shear tractions they will give rise to similar normal and shear displacements, and from this stems the results enabling us to write down the results showing how incomplete contact problems may be represented as distributions of flat faced punches, associated with the names Mossakovskii (1953) and Barber (1974). Turning the result the other way around, under conditions where the interface does not slip, changes in shear traction distribution will be proportional to changes in contact pressure.

^{*} Corresponding author.

E-mail address: james.truelove@eng.ox.ac.uk (J.P.J. Truelove).

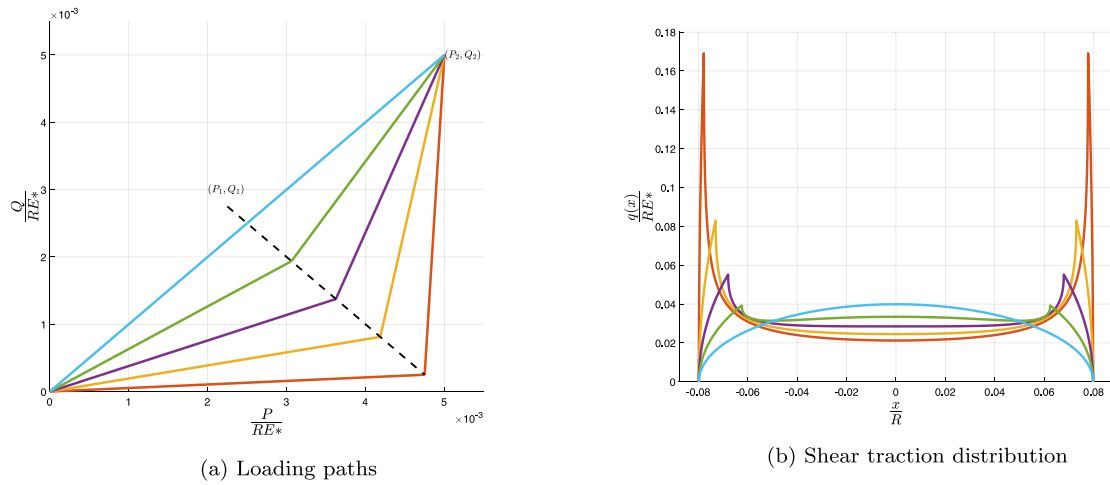


Fig. 1. Load paths and shear traction distributions for a fully stuck contact following a two piece straight line loading path.

2. Traction evolution during increasing normal load

In order to be able to write down the results of this analysis in a compact but universal way, Barber defined the following notation: suppose that the contact law, defining the contact half width, a in terms of the normal load, P , is simply $a(P)$. The notation $p(x; P)$ then gives the contact pressure distribution over the interval $-a \leq x \leq a$, and is zero outside this range. As an example, consider a Hertzian contact, where

$$a^2 = \frac{4PR}{\pi E^*}, \quad (2)$$

and here R is the relative radius of curvature of the contacting bodies and E^* is the plane strain composite elastic modulus for the contacting bodies. The contact pressure distribution is given by

$$p(x; P) \equiv \frac{2P}{\pi a} \sqrt{1 - \left(\frac{x}{a}\right)^2} \quad |x| < a(P). \quad (3)$$

If we consider forming of the contact from an unloaded state, and we do so by increasing the normal and shear forces in proportion, so that

$$\frac{dP}{P} = \frac{dQ}{Q} \quad (4)$$

and, if we think of this as applying an oblique force, the tangent of the angle between the loading direction and the contact normal, λ , is simply Q/P . When $\lambda < \mu$ the contact does not slide, and so there is no rigid body motion. But, in fact, because $q(x)/p(x) = \lambda$ the contact is fully stuck at all points.

It is illuminating, next, to look at problems where the contact has been loaded to the point (P_1, Q_1) , then loaded further, along a straight line in P - Q space to point (P_2, Q_2) , example load paths are shown in Fig. 1(a). The change in shear traction distribution going from 1 \rightarrow 2, assuming, for the time being, that it is fully stuck, is given by

$$\Delta q(x) = \frac{Q_2 - Q_1}{P_2 - P_1} [p(x; P_2) - p(x; P_1)] \quad (5)$$

and so

$$q_2(x) = \frac{Q_1}{P_1} p(x; P_1) + \frac{Q_2 - Q_1}{P_2 - P_1} [p(x; P_2) - p(x; P_1)]. \quad (6)$$

In interpreting these equations bear in mind that the pressure $p(x; P_i)$ is present over the interval $|x| < a_i$, and $a_2 > a_1$. Examples of the resulting shear traction distributions, for a Hertzian contact, ending up at the same point (Q_2, P_2) but with various intermediate points (Q_1, P_1) are shown in Fig. 1(b).

If $Q_2/P_2 < \mu$ the final contact will not be sliding, because it falls below the line $Q/P = \mu$. And, the change in traction ratio going from

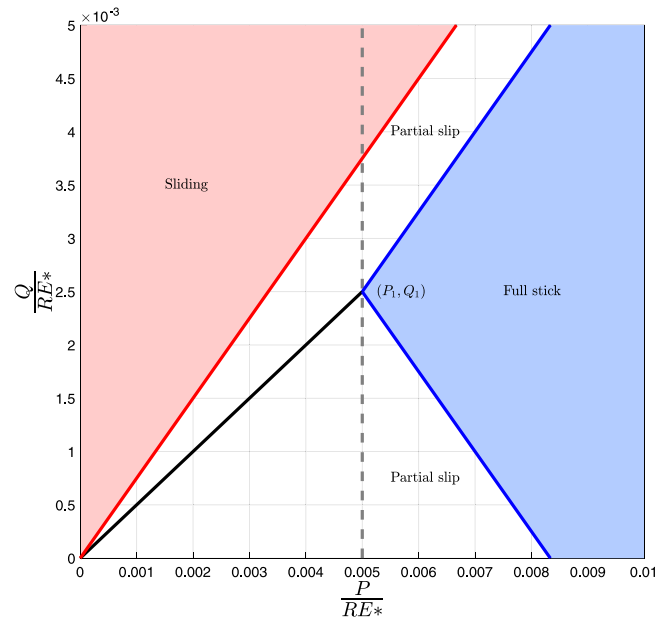


Fig. 2. A figure illustrating the various types of behaviour the contact can experience following various loading paths from the same point, in this case for a coefficient of friction of 0.75. The contact is first loaded proportionally under conditions of full stick to (P_1, Q_1) . If the contact is loaded under increasing normal load along a straight line to a point within the blue region the contact will remain fully stuck. If the contact is loaded into the red area the contact will slide. If the contact is loaded into the white regions then partial slip will occur. The gradients of the red and blue lines are the coefficient of friction. (For interpretation of the references to colour in this figure legend, the reader is referred to the web version of this article.)

1 \rightarrow 2 is given by (from (5))

$$\frac{\Delta q(x)}{\Delta p(x)} = \frac{Q_2 - Q_1}{P_2 - P_1} \quad a_1 < |x| < a_2. \quad (7)$$

If this ratio exceeds the coefficient of friction there will be regions of slip, i.e. the contact will be in partial slip, noting that here we are considering changes in the shear and normal load. This is illustrated in Fig. 2, if the second point lies inside blue the triangle shown the contact will remain fully stuck, if the second point lies within the red triangle the contact will be fully sliding, and if the second point is outside this region the contact will be in partial slip.

In cases where the gradient of the line exceeds the coefficient of friction the size of the slip zone will need to be found. This may be

done by making use of the result discovered independently by Jäger (1997, 1998) and Ciavarella (1998) that the requirement for stick to be preserved over a region $|x| < a_A$ when the actual contact size is $a_2 > a_A$ is given by

$$q(x) = \mu [p(x; P_2) - p(x; P_A)] \quad (8)$$

The shear traction is then given by

$$q_2(x) = \frac{Q_1}{P_1} p(x; P_A) + \mu [p(x; P_2) - p(x; P_A)] \quad (9)$$

and the value of P_A comes from the requirement of tangential equilibrium. It is the point of the initial loading trajectory defined by a line of gradient μ passing through point A, as shown in Fig. 3(a). Examples of the resulting shear traction distributions can be seen in Fig. 3(b), clearly demonstrating the varying size of stick zones resulting from different loading paths.

2.1. Normal load applied first and held constant

A special case of the above (and the one most frequently encountered in the literature), is when point 1 lies on the $Q = 0$ axis, and where $P_2 = P_1$. In this case the edge of the contact does not move during the loading phase $1 \rightarrow 2$, and in the limit, Eq. (5) takes a different form. For the case where the coefficient of friction is sufficient to prevent all slip the change in shear traction is given by,

$$\Delta q(x) = \frac{Q_2 - Q_1}{\pi \sqrt{a^2 - x^2}} \quad (10)$$

where $a_2 = a_1 = a$, as the normal load does not change during loading. Note that the shear traction here is singular (Fig. 4(a)), and is infinite at the edges of the contact, while for loading cases where the normal load increases while the shear increases the shear traction is bounded and tends to zero at the edge of the contact, even under conditions of infinite coefficient of friction. It is worth briefly discussing how this singular behaviour can arise from a bounded result.

Under conditions of full stick the change in shear traction moving from point 1 to point 2 is given by Eq. (5). To find the shear traction distribution under sequential loading we can consider the case where we load initially to a point $(P, 0)$, then further to a point $(P + \Delta P, Q)$ and take the limit where $\Delta P \rightarrow 0$

The change in shear traction moving from $(P, 0)$ to $(P + \Delta P, Q)$ is given by

$$\Delta q(x) = \frac{Q}{P - (P + \Delta P)} [p(x; P) - p(x; P + \Delta P)] \quad (11)$$

Which we then take the limit $\Delta P \rightarrow 0$

$$\Delta q(x) = Q \lim_{\Delta P \rightarrow 0} \frac{p(x; P + \Delta P) - p(x; P)}{\Delta P} \quad (12)$$

Where it should be noted that the second term is the definition of the derivative

$$f'(a) = \lim_{h \rightarrow 0} \frac{f(a + h) - f(a)}{h} \quad (13)$$

So that the change in shear traction becomes

$$\Delta q(x) = Q \frac{\partial p(x; P)}{\partial P} \quad (14)$$

Taking the example of a Hertzian Contact, the contact law given by Eqs. (2) and (3) can be written in the form

$$p(x, P) = \sqrt{\frac{PE^*\pi}{R} - \frac{x^2 E^*{}^2 \pi}{4R}} \quad (15)$$

Which has the derivative

$$\frac{\partial p(x; P)}{\partial P} = \frac{1}{\pi \sqrt{\frac{4PR}{E^*\pi} - x^2}} = \frac{1}{\pi \sqrt{a^2 - x^2}} \quad (16)$$

which leads us to Eq. (10). In more general terms it can be shown that the contact pressure immediately adjacent to the edge of any

incomplete contact is square root bounded in form, $p(s) = L_I \sqrt{s}$, where s is a coordinate set measured from the contact edge and L_I is an asymptotic multiplier. Changing the applied normal load changes the value of L_I and the location of the contact edge, but does not change the form of the pressure distribution. The derivative of the contact pressure is therefore square root singular in form, $\frac{dp}{ds} = \frac{K_I}{\sqrt{s}}$.

When slip is permitted the same principle for finding point A discussed in the section on two step loading continues to apply, and so by taking $P_2 = P_1$ and $Q_1 = 0$ we can state that in place of Eq. (9) we instead have

$$q_2(x) = \mu \left[p(x; P_2) - p(x; (P_2 - \frac{Q_2}{\mu})) \right] \quad (17)$$

which is the standard Jäger–Ciavarella solution (Fig. 4(b)).

3. Unloading

Let us now consider the behaviour of the contact when it is unloaded, so that the direction of shear loading *increment* is reversed. The instant the direction of shear loading changes the entire contact will stick, as the increment of shear traction across the entire contact violates the orthogonality requirement for frictional slip, and any slip that occurred during the previous loading will be locked into the resulting stick zone. Assuming that the *overall* magnitude of the applied shear load is small enough to avoid full sliding the contact will remain fully stuck if the gradient of unloading is less than the coefficient of friction, and the change in shear traction will be described by Eq. (5). If, however, the gradient of unloading is greater than the coefficient of friction then zones of slip in the opposite direction will appear, starting from the edge of contact. The solution for a contact with zones of slip at each end with a stuck central portion is given by a Ciavarella–Jäger type distribution, so that the solution to the shear traction is, therefore, a superposition of the shear traction distribution representing the locked in slip from the previous loading stage, and a Ciavarella–Jäger distribution of magnitude $-\mu$ representing the newly slipping regions. Consider the load path in Fig. 5(a). A contact that is loaded initially to point (P_1, Q_1) proportionally without slip, then loaded in an increasing manner further to point (P_2, Q_2) causing slip with stick zone associated with normal load P_A , then finally loaded under increasing normal load but decreasing shear to (P_3, Q_3) with associated slip zone size P_B . The shear traction distribution is given by

$$q_3(x) = \frac{Q_1}{P_1} p(x; P_A) + \mu [-p(x; P_3) + 2p(x; P_B) - p(x; P_A)] \quad (18)$$

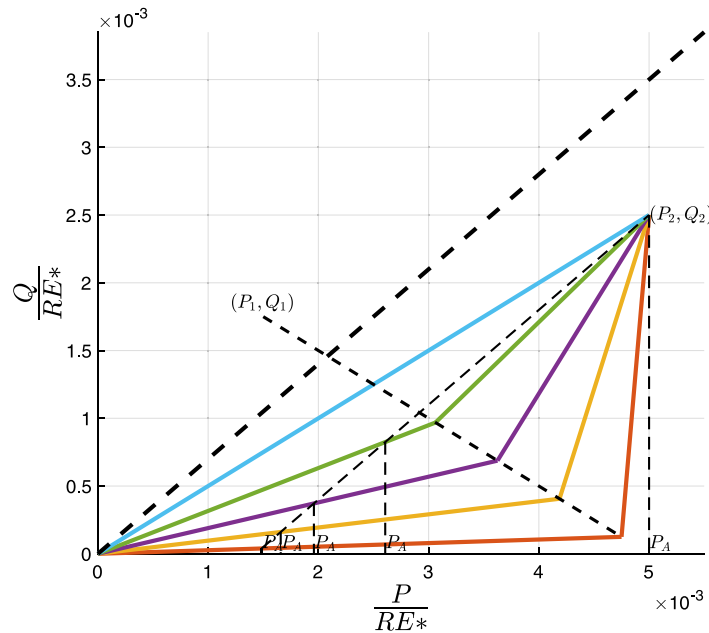
Where the $\frac{Q_1}{P_1} p(x; P_A)$ term represents the shear traction remaining from the proportional loading locked into the stick zone during the first stage of slip, $\mu [p(x; P_B) - p(x; P_A)]$ is the remaining shear traction distribution from the first stage of slip during loading, preserved over the stuck region during unloading, and $-\mu [p(x; P_3) - p(x; P_B)]$ is the shear traction distribution from the reverse slip during unloading, where the region between a_3 and a_B is now slipping in the reverse direction. These various shear tractions are shown in Fig. 5(b).

In this expression there is one unknown load, P_B , which can be found by considering horizontal equilibrium. Considering the total shear force due to each distribution in Eq. (18) we can write

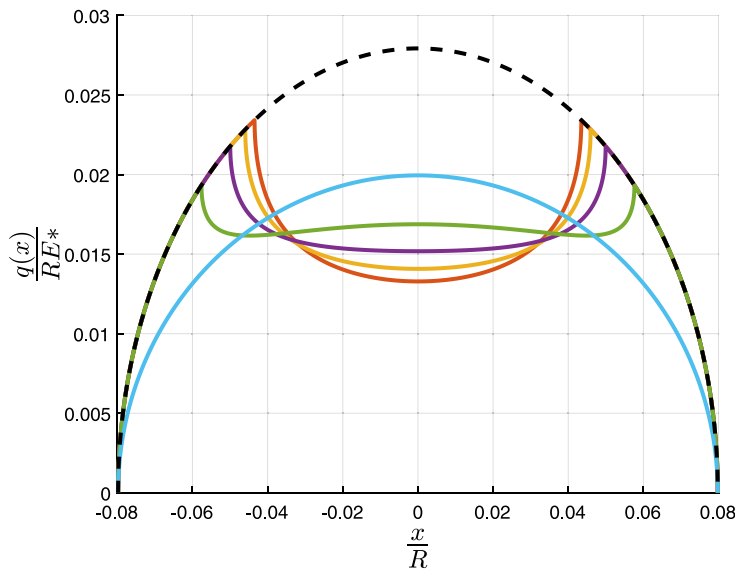
$$Q_3 = \frac{Q_1}{P_1} P_A - \mu P_3 + 2\mu P_B - \mu P_A \quad (19)$$

where we know the value of every term except P_B . Geometrically this expression is equivalent to finding the normal load at the intersection of a line of gradient $-\mu$ passing through (P_3, Q_3) and a line of gradient μ passing through point (P_1, Q_1) (i.e. the line used to define the point P_A). This construction is shown in Fig. 5(b).

The previous solution applies as long as the region of reverse slip during unloading is smaller than the region of slip during loading. If the region of reverse slip becomes larger than the slip zone during



(a) Loading paths and construction to find P_A , showing how the value of P_A (and therefore the size of the slip zone) depends upon the loading path.



(b) Shear traction distributions for the load paths in figure 3a, and the limiting shear traction $\mu p(x; P_2)$ (black, dashed)

Fig. 3. Load paths, geometric construction to find P_A and shear traction distribution for a two step loading with a frictional contact, showing the varying size of the slip zones under different loading paths (except light blue, which remains stuck everywhere). (For interpretation of the references to colour in this figure legend, the reader is referred to the web version of this article.)

the initial loading then the slip associated with the initial loading is completely erased, and the shear traction is instead given by

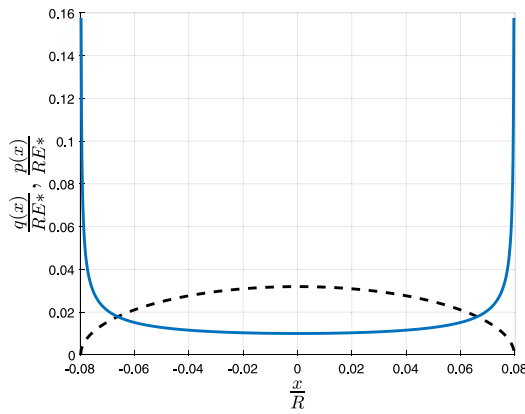
$$q_3(x) = \frac{Q_1}{P_1} p(x; P_C) + \mu [-p(x; P_3) + p(x; P_C)], \quad (20)$$

where the first term represents the shear traction from the initial loading path locked into the stick zone, and the second and third terms comprise a Ciavarella–Jäger type distribution corresponding to the region of reverse slip. The slip from the second stage of loading has, at this point, been entirely erased, and as such does not contribute to the shear traction distribution, note that the resulting shear traction is equivalent to a contact loaded straight to (P_3, Q_3) without the initial forward slip. The resultant shear traction is illustrated in Fig. 6(b).

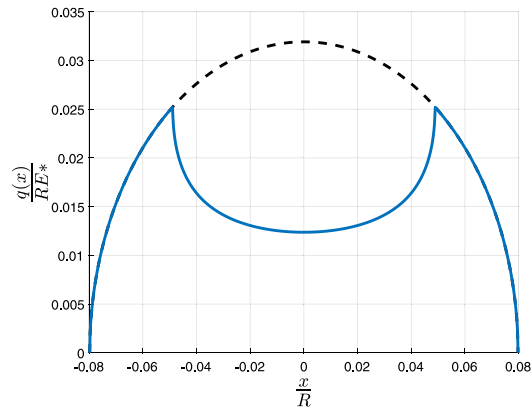
Once again we can find the value of the unknown load P_C by considering horizontal equilibrium of the entire contact. Once again considering the total shear loads transmitted by each component of Eq. (20) we can write

$$Q_3 = \frac{Q_1}{P_1} P_C - \mu P_3 + \mu P_C. \quad (21)$$

Geometrically this is equivalent to finding the normal load at the intersection of a line of gradient $-\mu$ passing through point (P_3, Q_3) and the initial loading line to (P_1, Q_1) , again this construction is illustrated in Fig. 6(a).

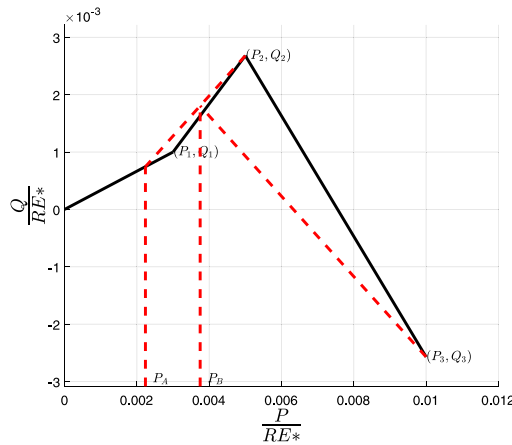


(a) The shear traction and pressure distribution for a sequentially applied loading with no slip

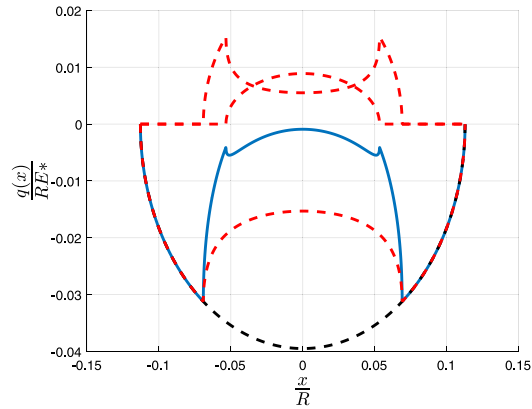


(b) The shear traction and limiting shear traction, $\mu p(x; P_2)$, for a sequentially applied loading with frictional interface. This is the standard Jäger-Ciavarella solution.

Fig. 4. Shear traction distributions for sequentially loaded contacts, under both full stick and partial slip conditions.



(a) The loading and unloading paths used in this problem, illustrating the constructions used to find the normal loads corresponding to the size of the stick zone during loading, P_A , and the size of the stick zone during unloading, P_B .



(b) The resultant shear traction, shown in blue, along with the limiting shear traction for slip (black, dashed) and the three shear traction distributions that make up the distribution, as discussed in the text.

Fig. 5. The loading paths and shear traction distributions for a contact that is initially loaded causing forward slip, then unloaded causing reverse slip, for the case where the region of reverse slip is smaller than the region of forward slip. (For interpretation of the references to colour in this figure legend, the reader is referred to the web version of this article.)

4. Cyclic loading

A form of loading that frequently occurs in engineered systems is one where the loading takes some initial path through P, Q space to a large value, then a smaller cyclic loading is superposed. This type of loading may occur, for example, in aero engines where a large centripetal force is developed by a fan blade during spin up, followed by a smaller vibrational load. Let us consider a contact under the following load path — the contact is initially loaded in a proportional manner to a point (P_i, Q_i) , and then repeatedly takes a straight line path between two other points in (P, Q) space, where (P_i, Q_i) lies on the path between them. A contact under this loading sequence has previously been studied by Fleury et al. (2017) by applying a simplified form of the results derived by Barber et al. (2011).

The resultant shear traction following the initial proportional loading to (P_i, Q_i) then (P_2, Q_2) can be found in a manner identical to that discussed in Section 2. The size of the stick zone during the initial load path is again given by the size of contact associated with normal load P_A , where P_A is found from the intersection of a line, passing through (P_2, Q_2) and with gradient μ with the initial load path. In the steady state the size of the permanent stick zone is given by the

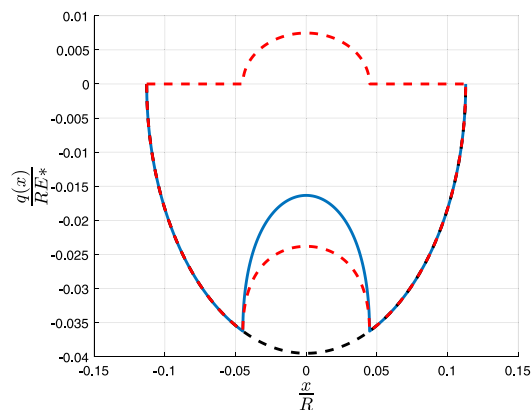
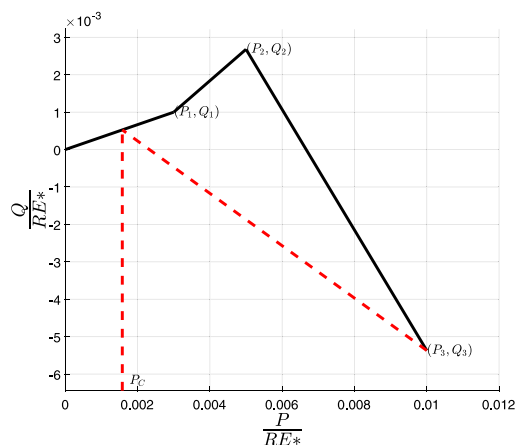
contact size associated with normal load P_K , where P_K is found from the intersection of a line with gradient μ passing through point (P_2, Q_2) , and a line of gradient $-\mu$ passing through point (P_1, Q_1) . This is shown in Fig. 8, which shows the constructions to find load P_A in dashed black lines, and the constructions to find point P_K in dashed red lines. There are therefore two possible regimes to consider, following some loading paths the steady state stick zone will be larger than the transient stick zone, so some slip will be permanently locked into the contact, while other loading paths will result in a steady state stick zone that is smaller than the transient one, so the slip during the initial phase of loading will be erased.

As discussed the initial stage of the problem, loading up to point (P_2, Q_2) is exactly equivalent to the two step loading problem already studied. At the end of loading the shear traction distribution is therefore given by

$$q_2(x) = \frac{Q_i}{P_i} p(x; P_A) + \mu [p(x; P_2) - p(x; P_A)] \quad (22)$$

where P_A is found from horizontal equilibrium,

$$P_A = \frac{Q_2 - \mu P_2}{\frac{Q_i}{P_i} - \mu} \quad (23)$$



(a) The loading path used for this contact and the contact, illustrating the construction used to find the value of normal load corresponding to the size of the stick zone during the unloading phase

(b) The resulting shear traction distribution for this loading path, shown in blue, along with the limiting shear traction in black and the two shear distributions that make up the overall shear traction, shown in red.

Fig. 6. The loading path, construction, and resultant shear traction distribution for a contact where the size of the stick zone during unloading is smaller than that present during loading. (For interpretation of the references to colour in this figure legend, the reader is referred to the web version of this article.)

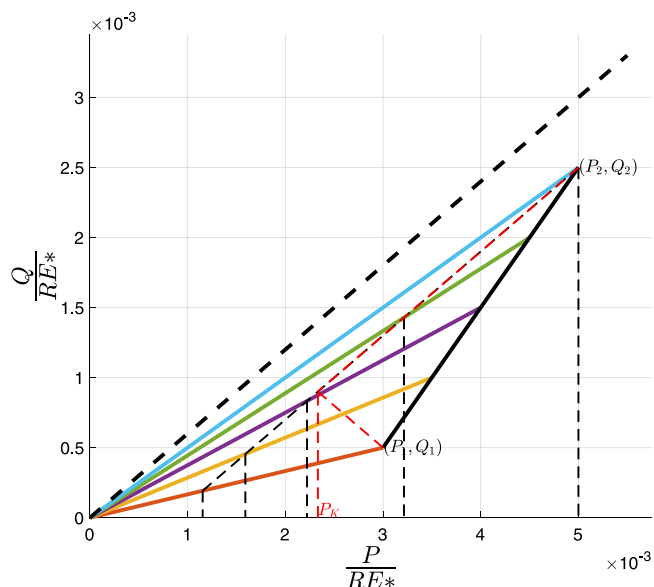
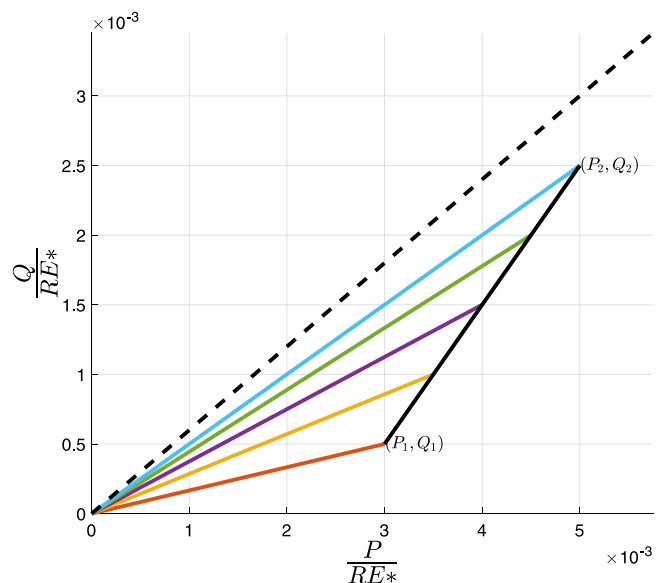


Fig. 7. The load path taken through our cyclic loading example. The contact is initially loaded in a proportional manner to a point (P_1, Q_1) following the various coloured paths. The contact is then further loaded to point (P_2, Q_2) , then cycled between (P_2, Q_2) and (P_1, Q_1) . Note that the gradient of the cyclic loading is greater than the coefficient of friction (black, dashed). (For interpretation of the references to colour in this figure legend, the reader is referred to the web version of this article.)

Fig. 8. The load paths taken in the cyclic loading example, overlaid with the constructions for finding the loads that correspond to the size of the stick zone during the initial loading (P_A , black) and the size of the steady state stick zone (P_K , red). (For interpretation of the references to colour in this figure legend, the reader is referred to the web version of this article.)

which is, once again, geometrically equivalent to the intersection of a line of gradient μ intersecting the initial loading line. Plots of the shear traction distributions at this point in the cycle for the load paths shown in Fig. 7 are shown in Fig. 9(a).

We now unload the contact to point (P_1, Q_1) along a straight path from (P_2, Q_2) . As discussed there are two possibilities to consider: if the steady state stick zone is larger than the transient stick zone ($P_K > P_A$) then the initial loading path will leave slip locked into the permanent stick zone. The solution to the shear traction is found by superimposing another Ciavarella-Jäger distribution on top of the existing shear traction distribution, giving

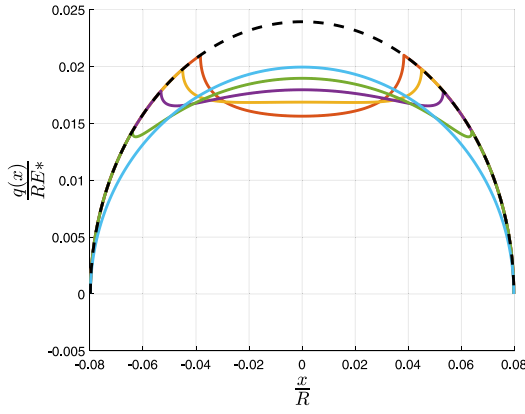
$$q_1(x) = \frac{Q_i}{P_i} p(x; P_A) + \mu [-p(x; P_1) + 2p(x; P_B) - p(x; P_A)], \quad (24)$$

where again P_R can be found through horizontal equilibrium,

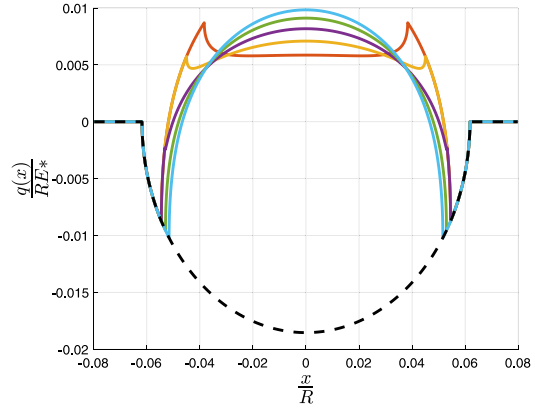
$$P_B = \frac{Q_1 - Q_A + \mu P_1 + \mu P_A}{2\mu}. \quad (25)$$

For the case where the steady state stick zone is smaller than the transient stick zone the slip that occurs during unloading will erase any slip that occurred during the initial loading to point 2. In this case the problem is identical to a contact that is loaded to (P_i, Q_i) then straight to (P_i, Q_i) , with the shear traction distribution given by

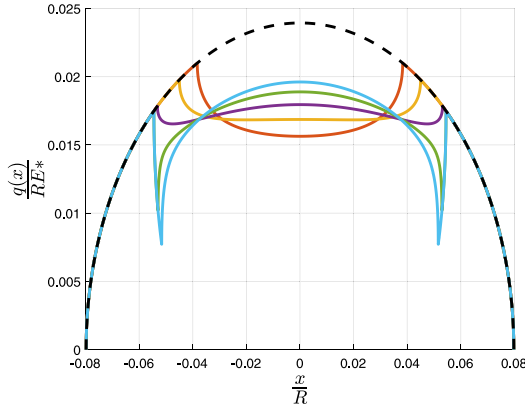
$$q_1(x) = \frac{Q_i}{P_i} p(x; P_C) - \mu [p(x; P_1) - p(x; P_C)]. \quad (26)$$



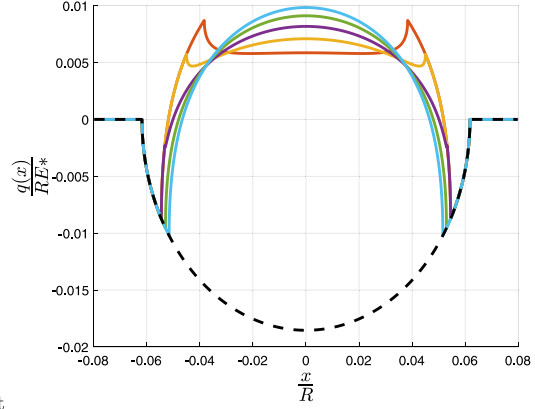
(a) The shear traction distributions following the initial loading to point (P_i, Q_i) then (P_2, Q_2) . This is found in an equivalent manner to the shear traction distribution found in section 2 for a two step loading cycle



(b) The shear traction distributions following unloading to (P_1, Q_1) . Note that in some of these loading paths the slip zone size during unloading is larger than the slip zone size during the initial loading to point (P_2, Q_2) , while for some paths the opposite is true



(c) The shear traction distribution following re-loading to point (P_2, Q_2) . The contact is now in the steady state portion of the loading cycle. Note that some of these shear traction distributions have regions within the permanent stick zone that reach contact has regions which reach the limiting coefficient of friction but which do not experience further slip displacement with further loading cycles



(d) The shear traction distribution following unloading to point (P_1, Q_1) . Again for certain load paths the stuck region of the contact has regions which reach the limiting coefficient of friction but which do not experience further slip

Fig. 9. Shear traction distributions for a Hertzian contact loaded through the path given in Fig. 7 at various points in the load cycle.

Note the change of sign of the second two terms, where P_C can again be found from horizontal equilibrium,

$$P_C = \frac{Q_1 + \mu P_1}{\frac{Q_1}{P_1} + \mu}. \quad (27)$$

This is the geometrically equivalent case to the intersection of a line of gradient $-\mu$ passing through (P_1, Q_1) and the initial loading path.

We now re-load the contact to (P_2, Q_2) . At this point in the load cycle there are, again, two possibilities to consider — the contact may have locked in slip from the initial loading to (P_2, Q_2) still present in the stick zone, or it may have been erased in the unloading cycle. When the loading is reversed the contact will initially stick everywhere, and a slip zone will grow from the outer edge of the contact. The solution is once again formed by superimposing a Ciavarella–Jäger distribution on top of the exiting shear distribution.

For the case where the slip zone from the initial loading cycle is still present in the stick zone, the resulting shear traction will be given by

$$q_2(x) = \frac{Q_i}{P_i} p(x; P_A) + \mu [p(x; P_2) + 2p(x; P_B) - p(x; P_A) - 2p(x; P_D)], \quad (28)$$

whereas for the case where the slip from the initial loading was erased by the reversing load the shear traction is given by

$$q_2(x) = \frac{Q_i}{P_i} p(x; P_C) + \mu [p(x; P_2) - p(x; P_C) - 2p(x; P_D)], \quad (29)$$

where once again we can find the value of P_D through horizontal equilibrium

$$P_D = \frac{-(Q_2 - Q_C - \mu P_2 - \mu P_C)}{2\mu} = P_B. \quad (30)$$

Note that the slip zone here does not extend into the stick zone that was present during the unloading stage, and so the slip locked into the stick zone remains unchanged.

Finally we unload the contact once again to (P_1, Q_1) . Once again the contact will stick everywhere initially, with slip zones growing in from the outer edges, so once again the solution is given by the superposition of a Ciavarella–Jäger distribution on top of the existing shear traction. Since there was no additional slip in the stick zone during the loading to (P_2, Q_2) horizontal equilibrium tells us that the slip zone will be the same size as that present during the initial unloading to (P_1, Q_1) . The solution to the stresses are therefore given by Eqs. (26) and (24), for

the cases where the slip zone during the first loading stage is locked into the steady state slip zone and erased respectively.

The solution has now reached its steady state, and any subsequent loading cycles will simply cause the state of stress to oscillate between the final two sets of equations. It is worth noting that the slip locked into the permanent stick zone means that there are regions of the permanent stick zone that reach the limiting coefficient of friction but which experience no further slip.

5. Conclusion

In this paper known solutions for the behaviour of a contact under various combinations of pressure and shear loading are given. The effect of various load paths are considered, and methods of finding the shear traction distribution through superposition are considered. The results given in this paper are applicable to any form of contact which can be represented by half planes, and the methods used to derive them can readily be extended to other loading histories.

CRediT authorship contribution statement

J.P.J. Truelove: Formal analysis, Investigation, Software, Validation, Visualization, Writing – original draft, Writing – review & editing. **L.E. Blades:** Supervision, Writing – review & editing. **D.A. Hills:** Conceptualization, Formal analysis, Funding acquisition, Project administration, Supervision, Writing – original draft, Writing – review & editing.

Declaration of competing interest

The authors declare that they have no known competing financial interests or personal relationships that could have appeared to influence the work reported in this paper.

Acknowledgements

James Truelove acknowledges with thanks the award of an iCASE award ref 17000027 from Rolls-Royce plc which has enabled him to carry out this work.

David Hills and Luke Blades acknowledge Rolls-Royce plc and the EPSRC, United Kingdom for their support under the Prosperity Partnership Grant “Cornerstone: Mechanical Engineering Science to Enable Aero Propulsion Futures”, Grant Ref: EP/R004951/1.

References

- Andresen, H., Hills, D.A., Barber, J.R., Vazquez, J., 2019. Frictional half-plane contact problems subject to alternating normal and shear loads and tension in the steady state. *Int. J. Solids Struct.* 168, 166–171.
- Andresen, H., Hills, D., Barber, J., Vázquez, J., 2020. Steady state cyclic behaviour of a half-plane contact in partial slip subject to varying normal load, moment, shear load, and moderate differential bulk tension. *Int. J. Solids Struct.* 182, 156–161.
- Barber, J., 1974. Determining the contact area in elastic-indentation problems. *J. Strain Anal.* 9 (4), 230–232.
- Barber, J., Davies, M., Hills, D., 2011. Frictional elastic contact with periodic loading. *Int. J. Solids Struct.* 48 (13), 2041–2047.
- Cattaneo, C., 1938. Sul contatto de due corpi elastici: Distribuzione locale degli sforzi. *Rend. Accad. Naz. Lincei* 27, 342–349.
- Ciavarella, M., 1998. The generalized Cattaneo partial slip plane contact problem. I Theory. *Int. J. Solids Struct.* 35 (18), 2349–2362.
- Fleury, R., Hills, D., Ramesh, R., Barber, J., 2017. Incomplete contacts in partial slip subject to varying normal and shear loading, and their representation by asymptotes. *J. Mech. Phys. Solids* 99, 178–191.
- Jäger, J., 1997. Half-planes without coupling under contact loading. *Arch. Appl. Mech.* 67 (4), 247–259.
- Jäger, J., 1998. A new principle in contact mechanics. *J. Tribol.* 120 (4), 677–684.
- Mossakovskii, V., 1953. Application of the reciprocity theorem to the determination of the resultant forces and moments in three-dimensional contact problems. *PMM* 17, 477–482.